MSL
ACADEMIC ENDEAVORS

Cleveland State University

EngagedScholarship@CSU

Physics Faculty Publications

Physics Department

12-1-2006

The Influence of the Sub-Cloud Moisture Field on Cloud Size Distributions and the Consequences for Entrainment

Harm J.J. Jonker
Delft University of Technology, h.jonker@ws.tn.tudelft.nl

Remco A. Verzijlbergh
Delft University of Technology

Thijs Heus
Delft University of Technology

A. Pier Siebesma
Royal Netherlands Meteorological Institute

Follow this and additional works at: https://engagedscholarship.csuohio.edu/sciphysics_facpub

Part of the Physics Commons

How does access to this work benefit you? Let us know!

2.4   THE INFLUENCE OF THE SUB-CLOUD MOISTURE FIELD ON CLOUD SIZE
DISTRIBUTIONS AND THE CONSEQUENCES FOR ENTRAINMENT.

Harm J.J. Jonker,[*]   Remco A. Verzijlbergh, Thijs Heus,
Dept. of Multi-Scale Physics, Delft University of Technology, The Netherlands
and A. Pier Siebesma, Royal Netherlands Meteorological Institute, The Netherlands

1. INTRODUCTION

Using Large Eddy Simulations of shallow cumulus clouds we analyse the relation between cloud-size and the fractional entrainment rate. First we determine the effect of fluctuations in the sub-cloud moisture field on the lateral size of clouds. To this end we apply at each time-step a spectral filter to the sub-cloud moisture field in order to prevent the formation of fluctuations with spatial scales that are significantly larger than the depth of the sub-cloud layer. The resulting cloud size distributions are compared to the unfiltered situation. Next, we focus on the impact on the cloud dynamics and on the depth of the cloud layer. In particular, we conduct a study of the lateral entrainment rate and analyse in detail its relation with the lateral size of clouds.

2. LES CASE DESCRIPTION AND METHODS

The Large Eddy Simulation is based on the Small Cumulus Microphysics Study (SCMS), held from July 17 till August 13 1995 near Cocoa Beach, Florida (Knight and Miller, 1998). An idealized LES version of the SCMS-case was created by Neggers et al. (2003) and includes a diurnal cycle by prescribing varying surface heat- and moisture-fluxes. In this study, the resolution is 50m in the horizontal and 40m in the vertical direction. With 128 points in each direction, the simulated domain is 6.4kmx6.4kmx5.1km. The entire run covered a 12-hr period and was simulated with a timestep of 2 seconds.

3. THE INFLUENCE OF THE SUB-CLOUD MOISTURE FIELD ON CLOUD SIZE DISTRIBUTIONS

Two types of LES have been conducted, a standard (reference) run and a simulation in which the large-scale fluctuations in the sub-cloud moisture field were removed, as done in Jonker et al. (1999). The filtering procedure consisted of spectrally removing fluctuations with scales larger than $1280m$ (about $2h$), see Fig. 1(b), where h is the depth of the sub-cloud layer. The filter was applied on all moisture fields with $z \leq 0.8h$, while taking into account that the sub-cloud layer grows during the simulation.

The main reason for filtering the sub-cloud moisture field was to be able to control the lateral size of the clouds, in particular to prevent the formation of relatively large

[*] *Corresponding author address:* Harm J.J. Jonker, Dept. of Multi-Scale Physics, Delft University of Technology, Lorentzweg 1, 2628CJ Delft, The Netherlands, e-mail: H.J.J.Jonker@tudelft.nl

clouds. It was expected that the filtered run, due to the absence of large clouds, would display a different dynamics and entrainment behaviour, which would then result in

(a)   (b)

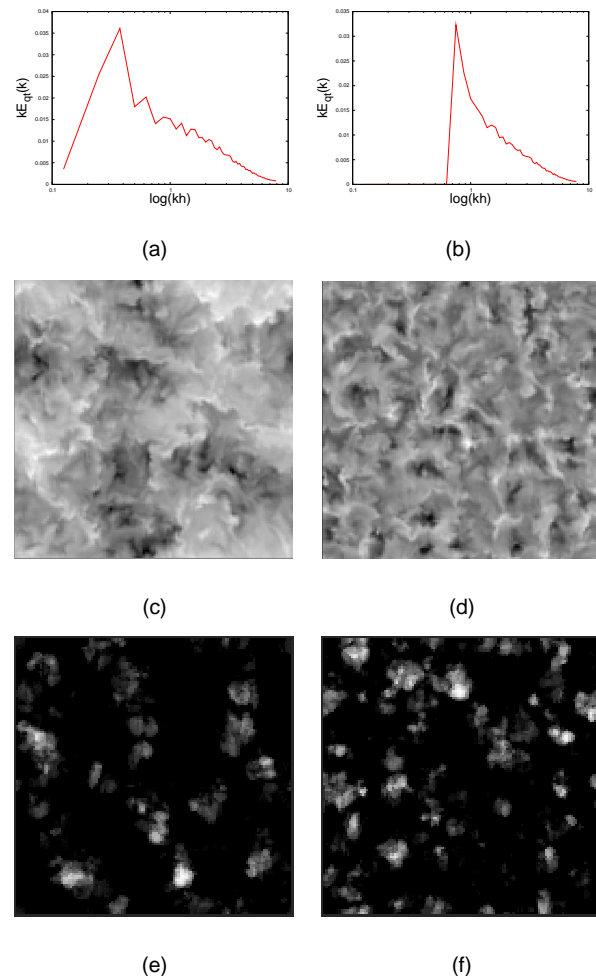(c)   (d)

(e)   (f)

FIG. 1: (a) Power spectrum from the unfiltered moisture field, 3 hour average from 18.00h to 21.00h UTC. (b) Power spectrum from the filtered run, scales larger then 1280m removed. (c) The cross-section of the moisture field at a height of 0.8 times the boundary-layer height h in the unfiltered run, approximately 18.00h UTC. (d) The sub-cloud moisture field in the filtered run, same cross-section height. (e) The cloud field as seen from a satellite at approximately 18.00h UTC. (f) Snapshot at the same time for the filtered run.

a different evolution of the cloud-top height compared to the reference run with large clouds.

Comparing Fig. 1(c) and Fig. 1(d) one can observe that the filter procedure worked properly to remove the large scale fluctuations from the sub-cloud moisture field. However, quite unexpectedly, the effects on the resulting cloud fields appear to be rather modest, as seen in Figs. 1(e),1(f) and in the cloud fraction profiles in Fig. 2. We emphasize that this result is in disagreement with the findings of Jonker et al. (1999). For some unknown reason the large clouds are missing in the reference case. The effect of filtering is therefore useless. Presumably the explanation for the lack of large clouds must be sought in the differences between the LES cases. Understanding this discrepancy may provide an interesting clue for the interaction between the cloud field and the sub-cloud moisture field, and the formation of (relatively) large clouds, but the issue is not pursued here.
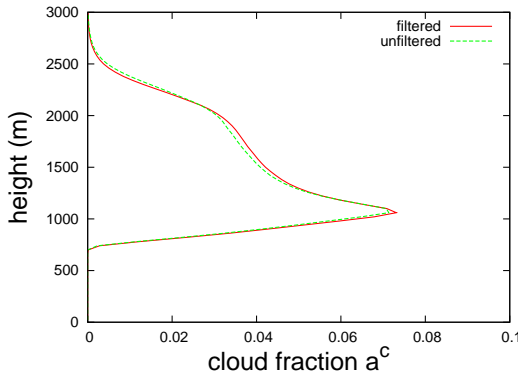

FIG. 2: Comparison of the cloud fraction between the filtered and unfiltered run. Clearly the effect of filtering is marginal.

4. THE RELATION BETWEEN CLOUD SIZE AND THE FRACTIONAL ENTRAINMENT RATE

A more direct way to study the relation between entrainment and cloud size is to calculate the fractional entrainment rate of cloud ensembles conditioned upon size, rather than of the entire ensemble as was done by e.g. Siebesma and Cuijpers (1995). To this end we calculated the volume V of each individual cloud in a simulated cloud field, and defined the (linear) size of the cloud by taking the cube root:

$$l = V^{\frac{1}{3}} \qquad (1)$$

We distinguished four classes based on size: $0 < l \leq 250$m, 250m$< l \leq 500$m, 500m $< l \leq 750$m, and $l > 750$m and calculated the entrainment and detrainment rates for each class separately. To obtain statistically reliable results, we conducted six independent LES runs (so called ensemble runs, with different random perturbations of the initial state) and additionally averaged the quantities over a three hour period.
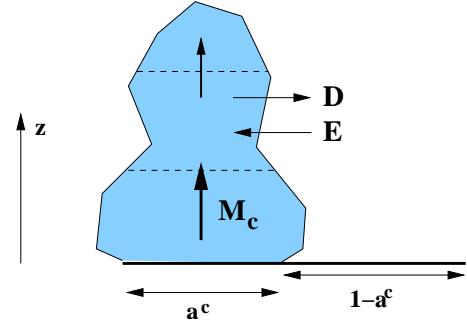

FIG. 3: Entrainment E and detrainment D in the mass-flux model

The entrainment and detrainment rates were derived with the mass-flux framework (Betts, 1973; Tiedtke, 1989), see Fig. 3.

$$\frac{\partial a^c}{\partial t} = -\frac{\partial M^c}{\partial z} + E - D \qquad (2)$$

with the cloud mass flux $M^c = a^c w^c$, w^c being the average upward velocity in the cloud. E and D represent the entrainment and detrainment rates respectively. The *fractional entrainment and detrainment rates* ε and δ are defined as

$$\varepsilon = \frac{E}{M^c} \qquad \delta = \frac{D}{M^c} \qquad (3)$$

Assuming steady state (2,3) become

$$\frac{1}{M^c}\frac{\partial M^c}{\partial z} = \varepsilon - \delta \qquad (4)$$

In many cloud and plume models, the mixing with the environment is described by the following 'simplified lateral mixing equation'

$$\frac{\partial \phi^c}{\partial z} = -\varepsilon(\phi^c - \phi^e) \qquad (5)$$

(e.g. Betts, 1975; Anthes, 1977; Tiedtke, 1989; Raga et al., 1990). The superscripts c and e represent cloud and environment, respectively. Here ϕ denotes a conserved quantity like q_t or θ_l.

The effective entrainment rate ε can be readily estimated by inverting equation (5) (e.g. Siebesma and Cuijpers, 1995) and using for example $\phi = q_t$. Hence we use the following equations to determine ε and δ

$$\varepsilon = -(q_t^c - q_t^e)^{-1}\frac{\partial q_t^c}{\partial z} \qquad \delta = \varepsilon - \frac{1}{M^c}\frac{\partial M^c}{\partial z} \qquad (6)$$

5. RESULTS

In Fig. 4 we show for different cloud sizes the profiles of total water $q_t(z)$, and liquid water $q_l(z)$ and in Fig. 5 the cloud fraction $a_c(z)$ and mass-flux $M_c(z)$. All graphs reveal a marked dependence on cloud-size. It is interesting to note that for the largest clouds, the cloud fraction is nearly constant with height and the mass-flux even increases. The implies that the average vertical velocity increases with height.
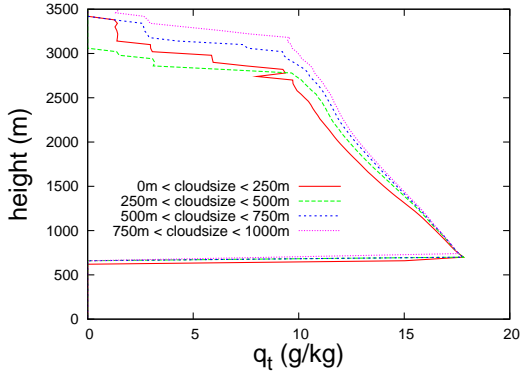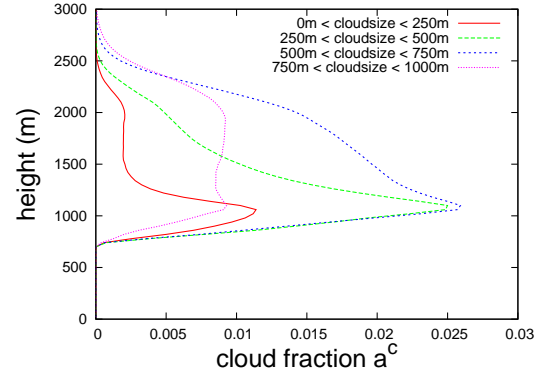
(a)
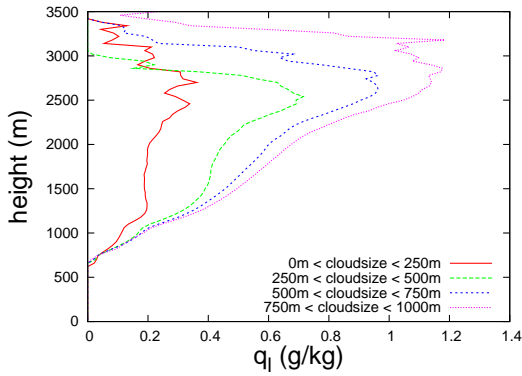
(b)

FIG. 4: Size decomposed vertical profiles of q_t, q_l and cloudfraction a^c. Note that the largest clouds have an approximately constant cloud fraction between 1000m and 2000m.
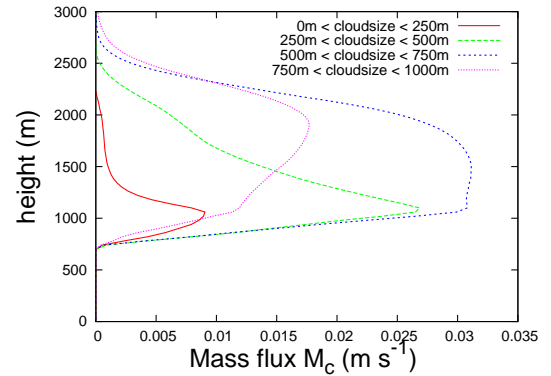

(a)

(b)

FIG. 5: Size decomposed vertical profiles of q_t, q_l and cloudfraction a^c. Note that the largest clouds have an approximately constant cloud fraction between 1000m and 2000m.

Using the results depicted in Figs. 4(a) and 5(b), we derived with equation (6) the entrainment and detrainment profiles for clouds of different sizes, see Fig. 6.

A first glance at the figure reveals that the entrainment rate indeed displays a dependence on cloud size, in particular for the smaller clouds. Regarding the detrainment rate, the same general picture seems to be present: There is an effect of size, but primarily for small clouds.

The size dependence of the entrainment rate has been further studied by decomposing the clouds in ten size categories, rather than four. To obtain a cloud size vs. entrainment relation, the average entrainment value in the region $z \in [1280, 2020]$m (this is the region where the graph is not so noisy and where forced clouds do not influence the statistics) has been calculated as function of cloud size. The results are depicted in Fig. 7. The first impression given above seems to hold: the entrainment rate shows a dependence on cloud size for sizes smaller than 500m. For clouds larger than this value, the entrainment rate appears to saturate.
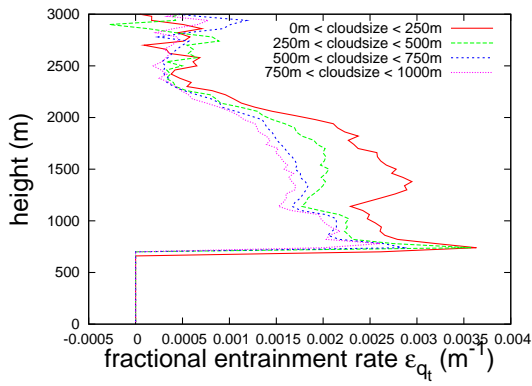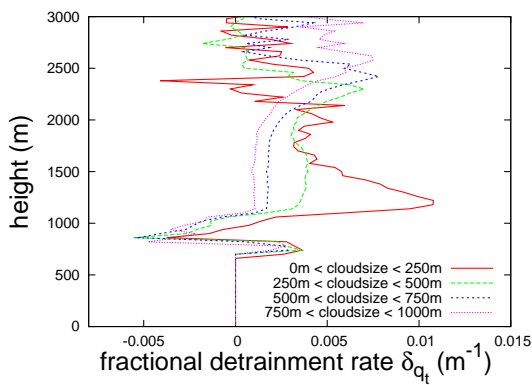
REFERENCES

Anthes, R., 1977: A cumulus parametrization scheme utilizing a one-dimensional cloud model. *Monthly Weather Review*, **105**, 270–286.

Betts, A. K., 1973: Non-precipating cumulus convection and its parametrization. *Quarterly Journal of the Royal Meteorological Society*, **99**, 178–196.

Betts, A. K., 1975: Parametric interpretation of trade-wind

(a)

(b)

Fɪɢ. 6: a) Entrainment profiles for four different sizes, b)detrainment profiles.

Fɪɢ. 7: Entrainment as function of cloud size. Values are averages over the region $1280m \leq z \leq 2020m$.

hawaii. *Journal of Atmospheric Sciences*, **47**, 338–355.

Siebesma, A. P. and J. Cuijpers, 1994: Evoluation of parametric assumptions for shallow cumulus convection. *Journal of Atmospheric Sciences*, **52**(6), 650–666.

Siebesma, A. P. and J. W. M. Cuijpers, 1995: Evaluation of parametric assumptions for shallow cumulus convection. *J. Atmos. Sci.*, **52**, 650–666.

Tiedtke, M., 1989: A comprehensive mass flux scheme for cumulus parametrization in large scale models. *Monthly Weather Review*, **177**, 1779–1800.

cumulus budget studies. *Journal of Atmospheric Sciences*, **32**, 2363–2382.

Jonker, H. J. J., P. G. Duynkerke, and A. P. Siebesma, 1999: Development of mesoscale fluctuations in cloud topped boundary layers. In *Proceedings of the 13th Symposium on Boundary Layer Turbulence, American Meteorological Society, Dallas, Texas,10-15 Jan., 1999*, AMS, 197–200.

Knight, C. A. and L. J. Miller, 1998: Early radar echoes from small, warm cumulus: bragg and hydrometeor scattering. *J. Atmos. Sci.*, **55**, 2974–2992.

Neggers, R. A. J., P. G. Duynkerke, and S. M. A. Rodts, 2003: Shallow cumulus convection: Validation of large-eddy simulation against aircraft and Landsat observations. *Quart. J. Roy. Meteor. Soc.*, **129**(593), 2671–2696.

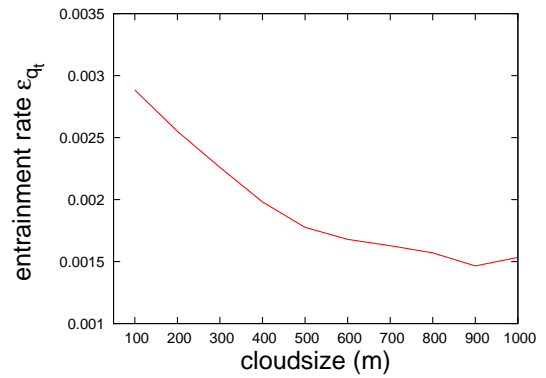Raga, G. B., J.B.Jensen, and M.B.Baker, 1990: Characteristics of cumulus band clouds off the coast of